and its application to circuit designs," *IEEE Trans. Electron Devices*, vol. ED-28, pp. 171–175, Feb. 1981.
[3] A Madjar. "Analysis of a microwave FET oscillator using an efficient computer model for the device," *IEEE Trans. Microwave Theory Tech.*, vol. MTT-30, pp 915–917, June 1982.
[4] H Abe, "Field-effect transistor ultra-high-frequency oscillator," Japanese patent, No. 51-6163, filed in Jan. 1976
[5] J Sone and Y. Takayama, "Equivalent circuit elements evaluation of GaAs MESFET," presented at National Conv. IECE, Japan, No. 104, Nov. 1976
[6] *Advanced Network Analysis Program*-6(ANAP-6), NEC Corporation User's Manual FXJ 12-3, Sept. 1977.

TM Modes in Oversized Planar Metallic Waveguides

DANIEL PASQUET, JEAN-LUC GAUTIER, AND PIERRE POUVIL

Abstract —**The propagation properties of transverse magnetic (TM) and hybrid modes in plane and circular metallic waveguides are considered when their dimensions are great with regard to the wavelength. When the oversizing is not too great, the behavior is the same as those of conventional metallic waveguides. For high frequencies (greater oversizing), we describe an unexpected behavior for these modes. The aim of this work is mainly to derive asymptotic expressions useful for the design of for infrared (FIR) waveguide lasers.**

I. Introduction

Oversized waveguides are used mainly in waveguide lasers. Indeed, the resonating modes always have low orders despite their large dimensions with regard to the wavelength. The waveguide constituting a laser cavity can be a dielectric or a metallic waveguide or both [1]. Its shape can be rectangular [1] or circular. The simplest propagating structure which is studied is the plane waveguide. J. J. Burke [2] has dealt with plane dielectric waveguides propagating TE modes. The propagation of TM modes in such guides are a little more complicated but can be studied rigorously [3]. Many authors have solved this problem for other frequency ranges [4], [7], especially for the Earth-ionosphere waveguide [4]–[6]. We have centered our work on the order of magnitude concerning the FIR lasers. Interesting approximate expressions can be carried out in that case [8] owing to the oversizing. Circular dielectric waveguide has been studied by E. A. J. Marcatili and R. A. Schmeltzer [9] in their well-known paper. The results for slab dielectric waveguides propagating TE and TM modes can be extended to circular dielectric waveguides propagating TE, TM, HE, and EH modes [10]. Metallic waveguides propagating TM and hybrid modes can be considered in the same way.

Plane metallic waveguides can propagate TE modes and TM modes. J. J. Burke's theory [2] is sufficient to describe TE modes. We only deal with TM modes. These modes have already been considered for different frequency bands.

Manuscript received April 8, 1985; revised July 18, 1985.
The authors are with Ecole Nationale Superieure de l'Electronique et de ses Applications, F95000 Cergy, France
IEEE Log Number 8405818.

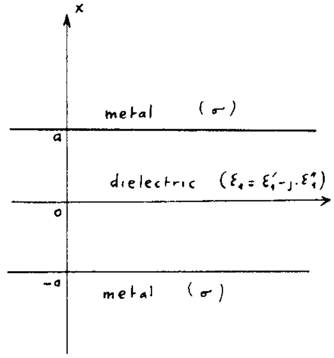

Fig. 1. Schematic description of a plane metallic waveguide.

II. Plane Propagation Structure

The propagating structure is shown in Fig. 1. A dielectric slab $2a$ thick with a permittivity ϵ_1 is bounded by two pieces of a metal which has a great conductivity σ. This medium can be considered with a permittivity that is equal to $j\sigma/\omega$, where ω is the angular frequency of the signal. The waveguide is infinite in the y and z directions and the fields are constant in y. As for dielectric waveguides, there are modes with either an even or odd variation of the transverse component of the electric field with respect to the transverse coordinate x. For all the modes, the generating function we have chosen is the longitudinal component E_z of the electric field.

III. Even TM Modes

For even TM modes, the E_z component has different expressions according to the medium in which it is considered. So, inside the dielectric medium $(-a < x < a)$

$$E_z = E_0 \sin \frac{ux}{a} \exp(-\gamma z) \exp(j\omega t) \quad (1)$$

in the metal

$$E_z = \pm E_0' \exp\left(\mp \frac{qx}{a}\right) \exp(-\gamma z) \exp(j\omega t). \quad (2)$$

The upper signs are for the upper metal $(x > a)$.

As in J. J. Burke's theory, the transverse wavenumbers u and q and the propagation constant γ are linked by

$$u^2 = (\mu_0 \epsilon_1 \omega^2 + \gamma^2) a^2 \quad (3)$$

$$q^2 = (-j\mu_0 \sigma \omega - \gamma^2) a^2 \quad (4)$$

$$R^2 = u^2 + q^2 = \mu_0 \omega (\epsilon_1 \omega - j\sigma) a^2 \quad (5)$$

where μ_0 is the permeability of the vacuum. The propagation constant has a real part α (attenuation) and an imaginary part β. The boundary conditions at the interfaces between dielectric and metallic media $(x = a$ and $x = -a)$ allow us to know the relation between the amplitude constants E_0' and E_0

$$E_0' = E_0 \sin u \exp q \quad (6)$$

and particularly the characteristic equation

$$\epsilon_1 q = -\frac{j\sigma}{\omega} u \tan u. \quad (7)$$

Equations (5) and (7) can be solved by the means of a desktop computer. Figs. 2 and 3 show the variations of the real and the imaginary parts u' and u'' of the inner transverse wavenumber u

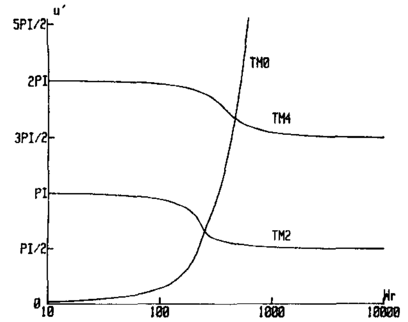

Fig. 2. Variation of the real part u' of the inner wavenumber u versus normalized frequency ($\sigma = 1.5 \times 10^7\ \Omega^{-1}\ \mathrm{m}^{-1}$, $\epsilon_1 = \epsilon_0$) for the first even TM modes.

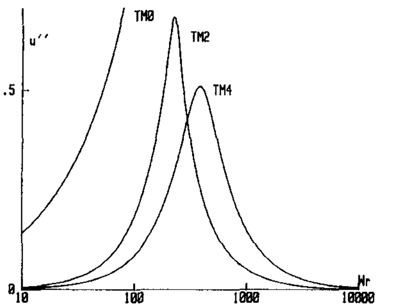

Fig. 3. Variation of the imaginary part u'' of u for the first even modes versus normalized frequency.

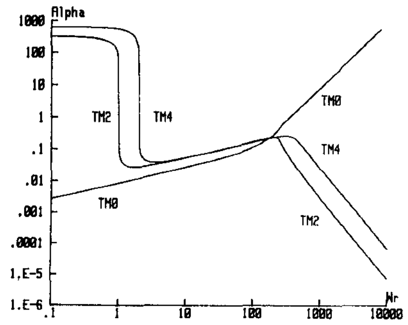

Fig. 4. Variation of the attenuation α for the first even modes versus normalized frequency.

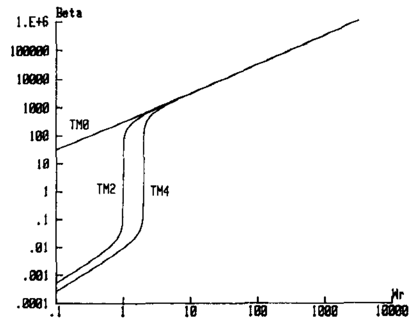

Fig. 5 Variation of the propagation constant β for the first even modes versus normalized frequency.

with regard to the frequency. The abscissa coordinate is normalized to 1 for the cutoff frequency of the TM_2 mode with perfect metal.

In these figures, the TM_0 mode does not have the same behavior as the other even TM modes so we will consider it separately. Two frequency regions appear for all the modes. For the lower frequencies, u is close to $N\pi/2$ for the TM_N modes and it is close to $(N-1)\pi/2$ for the higher frequencies. Using (3), the real and imaginary parts of γ can be computed and drawn as in Figs. 4 and 5.

For the very low frequencies, the well-known characteristics of metallic waveguides can be seen. Particularly, a cutoff frequency f_c can be defined by the equality between α and β

$$f_c = \frac{N+1}{4a\sqrt{\mu_0 \epsilon_1'}}. \tag{8}$$

For lower frequencies (but over $2f_c$), an asymptotic expression of u can be carried out with σ very large ($\sigma/\omega\epsilon_0 \gg 1$ and $\sigma\lambda_0^2/a^2\omega\epsilon_0 \gg 1$)

$$u \approx \frac{N\pi}{2} + (j-1)\frac{\sqrt{2\mu_0}\,\epsilon_1 a \omega^{3/2}}{N\pi\sqrt{\sigma}}. \tag{9}$$

It is also easy to obtain asymptotic expressions for α and β

$$\alpha \approx \frac{\omega\sqrt{\mu_0}\,\epsilon_1''}{2\sqrt{\epsilon_1'}} + \frac{\sqrt{\epsilon_1'\omega}}{a\sqrt{2\sigma}} \tag{10}$$

$$\beta \approx \omega\sqrt{\mu_0\epsilon_1'} - \frac{N^2\pi^2}{8a^2\omega\sqrt{\mu_0\epsilon_1'}} \tag{11}$$

where ϵ_1' and $-\epsilon_1''$ are the real and imaginary parts of the permittivity ϵ_1.

As can be seen in Fig. 4, α in this frequency region does not depend on the order of the mode. The second term of β, called the dispersion term, is the same as in the case of dielectric waveguides.

For higher frequencies, ω is now considered as very large ($\sigma/\omega\epsilon_0 \gg 1$ but $\sigma\lambda_0^2/a^2\omega\epsilon_0 \ll 1$)

$$u \approx \frac{(N-1)\pi}{2} + (1+j)\frac{(N-1)\pi\sqrt{\sigma}}{2\sqrt{2\mu_0}\,\omega^{3/2}a\epsilon_1} \tag{12}$$

which leads to

$$\alpha \approx \frac{\omega\sqrt{\mu_0}\,\epsilon_1''}{2\sqrt{\epsilon_1'}} + \frac{(N-1)^2\pi^2\sqrt{\sigma}}{4\sqrt{2}\,\mu_0\epsilon_1'^{3/2}\omega^{5/2}a^3} \tag{13}$$

$$\beta \approx \omega\sqrt{\mu_0\epsilon_1'} - \frac{(N-1)^2\pi^2}{8a^2\omega\sqrt{\mu_0\epsilon_1'}}. \tag{14}$$

The attenuation now decreases with the frequency. The cause of this is the deconfining of the propagated energy when u' decreases, i.e., when the frequency increases. The boundary between these two behaviors is defined by the angular frequency ω_T

$$\omega_T = \left[\frac{N(N-1)\pi^2\sigma}{4\mu_0 a^2\epsilon_1'^2}\right]^{1/3}. \tag{15}$$

For few centimeter-width waveguides, this angular frequency is situated between infrared and far infrared (wavelengths of few tens micrometers).

IV. Quasi-TEM (TM_0) Mode

As we have seen in the previous section, the TM_0 mode does not have the same behavior with regard to the frequency as the other even modes. For the lower frequencies, we recognize the usual TEM mode for perfect metallic waveguides. It has no cutoff frequency and the transverse inner wavenumber is close to

$$u \approx \epsilon_1'^{3/4}\mu_0^{1/4}\omega^{3/4}\sigma^{-1/4}a^{1/2}\exp\frac{3\pi j}{8} \tag{16}$$

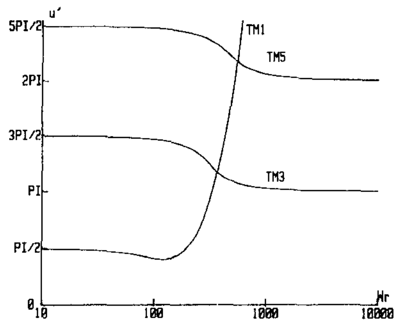

Fig. 6. Variation of the real part u' of u for the first odd modes versus normalized frequency.

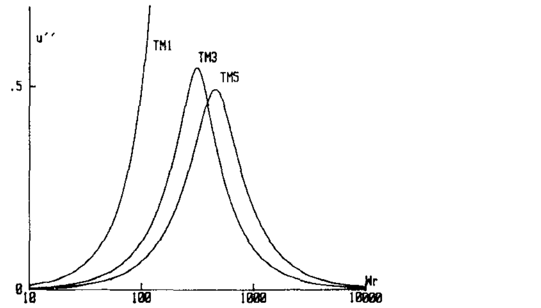

Fig 7 Variation of the imaginary part u'' of u for the first odd modes versus normalized frequency.

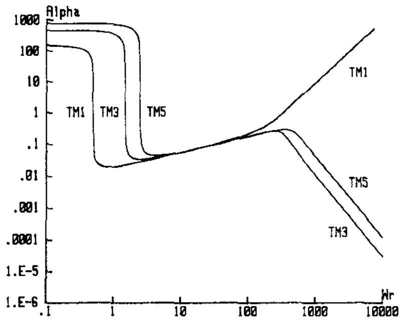

Fig. 8 Variation of the attenuation α for the first odd modes versus normalized frequency.

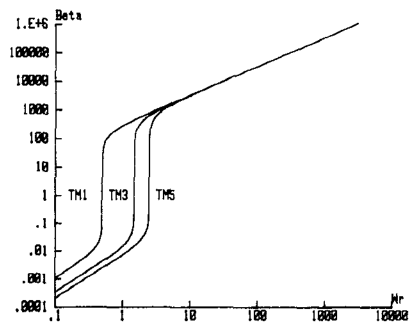

Fig. 9. Variation of the propagation constant β for the first odd modes versus normalized frequency

the attenuation is

$$\alpha \approx \frac{\omega\sqrt{\mu_0}\,\epsilon_1''}{2\sqrt{\epsilon_1'}} + \frac{\sqrt{\epsilon_1'\omega}}{a\sqrt{8\sigma}} \tag{17}$$

and the propagation constant is

$$\beta \approx \omega\sqrt{\mu_0\epsilon_1'} + \frac{\sqrt{2\epsilon_1'\omega}}{2a\sqrt{\sigma}}. \tag{18}$$

The existence of a dispersion term proves that it is not an exact TEM mode. It is the reason why we have called this mode the quasi-TEM mode.

For higher frequencies, the inner transverse wavenumber is close to

$$u \approx (1+j)\frac{\epsilon_1'\mu_0^{1/2}\omega^{3/2}a}{\sqrt{2\sigma}}. \tag{19}$$

The attenuation becomes very large

$$\alpha \approx \frac{\omega\sqrt{\mu}\,\epsilon_1''}{2\sqrt{\epsilon_1'}} + \frac{\epsilon_1'^{3/2}\sqrt{\mu_0}\,\omega^2}{2\sigma} \tag{20}$$

The variations of all the characteristics with regard to the frequency appear in Figs. 2–5 with the other TM even modes.

The boundary between the two ranges of frequency, defined by the equality between the approximate values of u'' with the two approximations is the angular frequency ω_T

$$\omega_T = \left(\sin\frac{3\pi}{8}\sqrt{2}\,\frac{\sigma^{1/4}}{\epsilon_1'^{1/2}\mu_0^{1/4}a^{1/2}}\right)^{4/3}. \tag{21}$$

If we consider that the increase of the frequency causes a deconfining of the propagated energy, all the transmission tends to approach the walls and increases the attenuation. When the frequency becomes higher, the propagation occurs more and more in the metal and no energy remains in the middle of the waveguide to ensure an almost lossless propagation.

V. Odd TM Modes

For odd TM modes, the expressions of E_z are the following in the dielectric:

$$E_z = E_0 \cos\frac{ux}{a}\exp(-\gamma z)\exp(j\omega t) \tag{22}$$

and in the metal

$$E_z = E_0'\exp\left(\mp\frac{qx}{a}\right)\exp(-\gamma z)\exp(j\omega t). \tag{23}$$

The upper sign is for $x > a$.

The boundary conditions give

$$E_0' = E_0 \cos u \exp q \tag{24}$$

and the characteristic equation

$$\epsilon_1 q = \frac{j\sigma u}{\omega \tan u}. \tag{25}$$

The simultaneous solution of (5) and (25) gives the curves as shown in Figs. 6 and 7.

The behavior of these modes for the lower frequencies is the same as those of the even TM modes (except TM_0). All the approximate expressions remain valid.

For the higher frequencies, the TM_1 mode is similar to the TM_0 mode, and the other odd TM modes, to the higher order even TM modes. So, each kind of relation for even modes remain valid for the appropriate odd modes.

Figs. 8 and 9 show the computed values of α and β. They confirm the similarity between the even and odd TM modes.

VI. Conclusion

The behavior of TM modes in plane metallic waveguides are quite different according to the frequency range.

For the lower frequencies, these modes are similar to those of the usual metallic waveguides. The TEM mode becomes TM_0 or a quasi-TEM mode. The other modes keep their properties. In particular, the attenuation varies like the square root of the frequency and the inverse of the dimension.

For higher frequency, the behavior of the modes are more unexpected. The TM_0 and TM_1 modes become very attenuated (the attenuation varies like ω^2). To the contrary, the other modes are far less attenuated (the attenuation varies like $\omega^{-5/2}$ and a^{-3}). This can be explained by the existence of central densities of energy, which only remain when the frequency increases. For TM_0 and TM_1 modes, this central density does not exist and these modes can't propagate any more for higher frequencies.

Our results can be used for the mixed rectangular metallic and dielectric waveguides [1], where quasi-LSE or quasi-LSM modes can be considered TE or TM modes with regard to the dielectric, and TM or TE modes with regard to the metal. The increase of the attenuation with the frequency for some low-order modes explains the poor Q coefficient for metallic cavities with respect to dielectric cavities. The same results can be obtained for circular metallic waveguides. Asymptotic expressions can be easily carried out.

References

[1] M. R. Schubert, M. S. Durschalg, and T. A. DeTemple, "Diffraction limited cw optically pumped laser," *IEEE Quantum Electron.*, vol. QE-13, pp. 455–459, 1977.
[2] J. J. Burke, "Propagating constants of résonant waves on homogeneous isotropic slab waveguide," *Appl. Opt*, vol. 9, pp. 2444–2452, 1970.
[3] D. Pasquet, "Accurate graphic resolution of the characteristic equation of a hollow dielectric slab waveguide," *Int. J. Infrared Millimeter Waves*, vol. 2, pp. 453–463, 1981.
[4] J. R. Wait and K. P. Spies, *Pure Appl. Geophys*, vol. 102, pp. 174–188, 1972.
[5] J. N. Polky and G. L. Mitchell, "Metal clad planar dielectric waveguide for integrated optics," *J. Opt. Soc. Amer.*, vol. 64, pp. 274–279, 1974.
[6] K. G. Budden and M. Eve, "Degenerate modes in the Earth-Ionosphere waveguide," *Proc. Roy. Soc. London*, vol. A342, pp. 175–190, 1975.
[7] Y. N. Lazarenko, V. F. Pavlov, and V. D. Sakhatskiey, "On some properties of surface waves in lossy media," *Radio Eng. Electron. Phys.*, vol. 21, pp. 118–120, 1976.
[8] B. Adam and F. Kneubühl, "Transversely excited 337-μm HCN waveguide laser," *Appl. Phys.*, vol. 8, pp. 282–295, 1975.
[9] E. A. J. Marcatili and R. A. Schmeltzer, "Hollow metallic and dielectric waveguides for long distance optical transmission and laser," *Bell Syst. Tech. J.*, vol. 43, pp. 1783–1809, 1964.
[10] D. Pasquet, "Waveguide discrete modes in slab and cylindrical FIR laser," *Int. J. Infrared Millimeter Waves*, vol. 2, pp. 1151–1163, 1981.

Response of Waveguides Terminated in a Tapered Metallic Wall

J. M. REBOLLAR

***Abstract*—The characteristics of waveguides terminated in a tapered metallic wall are analyzed by means of the modal analysis and scattering matrix concept of discontinuities. Several applications of this kind of termination are suggested. The results can be very useful in evaluating the phase errors produced due to the use of a short-circuited waveguide with a metallic wall not placed in an exact transverse plane (z = constant).**

Manuscript received May 17, 1985; revised August 6, 1985.
The author is with the Departamento de Teoria Electromagnetica, E.T.S.I. Telecommunication, Universidad Politecnica de Madrid, Ciudad Universitaria, 28040 Madrid, Spain.
IEEE Log Number 8405932.

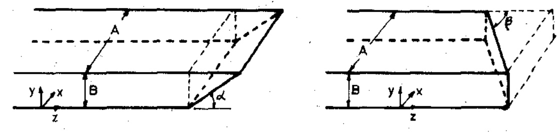

Fig. 1. Rectangular waveguides terminated in tapered metallic wall. (a) Type-"a" short circuit, slope α. (b) Type-"b" short circuit, slope β.

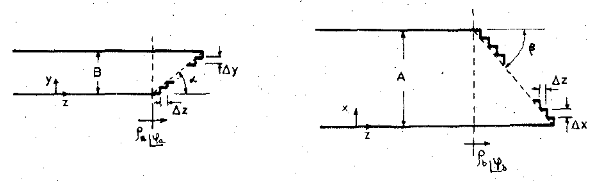

Fig. 2. Step-ladder modeling type-"a" and type-"b" short circuits, respectively.

I. Introduction

The classical way of terminating a waveguide with a metallic wall, to obtain a short circuit, is to place it in a transverse plane of the waveguide (plane z = constant). Different modes of the incident field are not generated by this termination, and the behavior of this short-circuited waveguide is well known.

However, the metallic wall can be placed, by error or by necessity, in an oblique plane.

In this paper, the effects of this kind of short circuit are studied. Two different terminations considered here are illustrated in Fig. 1(a) and (b).

II. The Model and Analysis Method

The geometry presented in Fig. 1 can be modeled by means of a step-ladder as it is shown in Fig. 2. As the steps get smaller in the limit, this model simulates properly the tapered metallic wall.

The geometries illustrated in Fig. 2 show N different waveguide sections of Δz length, terminated in a classical short circuit with metallic wall in a transverse plane.

These configurations can be exactly analyzed by means of a new technique combining the model analysis and scattering matrix concept of transverse discontinuities [1]–[3]. The electromagnetic field in each waveguide section is assumed to be the sum of their eigenmodes. Then the scattering matrix S of each discontinuity is obtained [3]. Finally, all discontinuities are joined in order to obtain the exact response of the complete structure by a method similar to that proposed by Patzelt and Arndt [3]. This method permits the combination of as many discontinuities as desired. The number of modes used to describe the electromagnetic field in each waveguide section can be as large as permitted by the computer. However, convergence is quickly obtained and 20 modes are enough to solve the problem.

The exciting field from the left is considered to consist of the fundamental TE_{10} mode of the rectangular waveguide. With this incident field, and considering the step discontinuities of the "a" and "b" cases, the next modes are considered.